

# Redox Brightening of Colloidal Semiconductor Nanocrystals Using Molecular Reductants

Jeffrey D. Rinehart, Amanda L. Weaver, and Daniel R. Gamelin\*

Department of Chemistry, University of Washington, Seattle, Washington 98195-1700, United States

**S** Supporting Information

**ABSTRACT:** Chemical reductants of sub-conduction-band potentials are demonstrated to induce large photoluminescence enhancement in colloidal ZnSe-based nanocrystals. The photoluminescence quantum yield of colloidal Mn<sup>2+</sup>-doped ZnSe nanocrystals has been improved from 14% to 80% simply by addition of an outer-sphere reductant. Up to 48-fold redox brightening is observed for nanocrystals with lower starting quantum yields. These increases are quickly reversed upon exposure to air and are temporary even under anaerobic conditions. This redox brightening process offers a new and systematic approach to understanding redox-active surface “trap states” and their contributions to the physical properties of colloidal semiconductor nanocrystals.

The redox chemistries of colloidal semiconductor nanocrystals (NCs, or quantum dots, QDs) remain relatively unexplored. Many studies have focused on the challenges of introducing and characterizing extra delocalized bandlike charge carriers.<sup>1–4</sup> Nanocrystal surfaces are also often redox-active, but surface “traps” have proven difficult to characterize despite their ability to influence many physical properties of the target QDs. For example, midgap surface traps can strongly suppress the excitonic photoluminescence (PL) of colloidal QDs<sup>5–11</sup> or compromise the transport properties of QD solids.<sup>12</sup> Controlling such traps thus represents a long-standing challenge in nanocrystal research. The most successful routes to surface-trap passivation have involved shell growth to provide spatial separation of the carriers from the surface<sup>6,11,13–15</sup> without necessarily eliminating the traps themselves. In some cases, binding of electron-rich ligands appears to have enhanced the ensemble PL and reduced single-particle blinking.<sup>16–21</sup> Electrochemical measurements on single CdSe-based nanocrystals on electrode surfaces have demonstrated reduced blinking under cathodic bias, attributed to electron trap filling.<sup>22–24</sup> We recently reported the reversible electrochemical passivation of electron traps in wide-gap ZnSe and Mn<sup>2+</sup>-doped ZnSe (Mn<sup>2+</sup>:ZnSe) NC films, which yielded strongly enhanced ensemble PL (“electrobrightening”).<sup>25</sup> As in the blinking studies, the microscopic origins of this brightening remain unclear, and in particular, it is important to determine whether this phenomenon is limited to NCs on electrode surfaces or if it is truly a property of the freestanding colloidal NCs.

Redox passivation of the surface traps of colloidal QDs would address this ambiguity and perhaps facilitate identification of the microscopic origins of this brightening by enabling chemical

analysis of the redox-active traps themselves using techniques that are incompatible with electrode surfaces. Electrochemistry on the freestanding colloidal QDs poses several daunting challenges, however, including the lack of a uniform potential throughout the solution and diffusive reoxidation at the counter electrode. Such challenges can be circumvented using a purely chemical approach. Here we demonstrate large increases in the PL quantum yields of colloidal Mn<sup>2+</sup>:ZnSe NCs through the controlled addition of midgap electrons via molecular electron shuttles. Mn<sup>2+</sup>:ZnSe NCs are described here for practical reasons, because the large energy shift between absorption and PL facilitates the measurements, but the underlying electron-trapping phenomenon is the same for undoped ZnSe NCs.<sup>25</sup>

Colloidal trioctylphosphine oxide (TOPO)-capped Mn<sup>2+</sup>:ZnSe NCs were prepared as described previously [see the Supporting Information (SI)]. To study traps, our first experiments were performed on NCs with deliberately small PL quantum yields ( $\phi = 0.4\%$ ). Initial attempts at reductive passivation of the surface traps on these NCs involved the addition of sodium–potassium alloy (NaK<sub>2</sub>) to stirred  $1.3 \times 10^{-6}$  M NC suspensions in tetrahydrofuran (THF) under an inert atmosphere. The addition of NaK<sub>2</sub> indeed induced PL brightening (Figure 1), but only after a long (~1 h) induction period. After a maximum of ~25-fold brightening was reached,

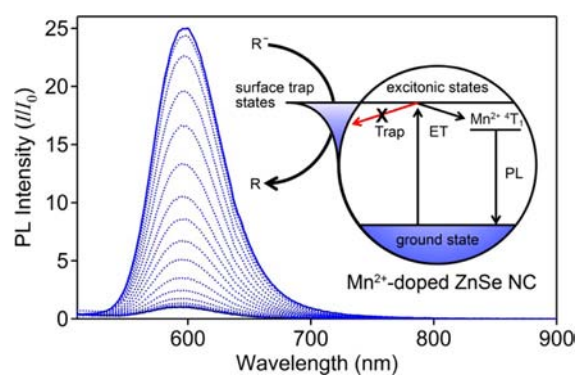


**Figure 1.** PL increase due to reductive passivation of surface traps in 0.6% Mn<sup>2+</sup>:ZnSe nanocrystals ( $1.3 \times 10^{-6}$  M;  $d = 4.6$  nm) under 405 nm excitation. PL intensities ( $I$ ) are normalized to the original intensity ( $I_0$ ). Inset: schematic of the redox process leading to PL enhancement. R is a reductant. Arrows illustrate nonradiative electron trapping (Trap) and energy transfer (ET) from the exciton to excite Mn<sup>2+</sup> into its <sup>4</sup>T<sub>1</sub> state, from which the PL occurs.

Received: August 10, 2012

Published: September 17, 2012

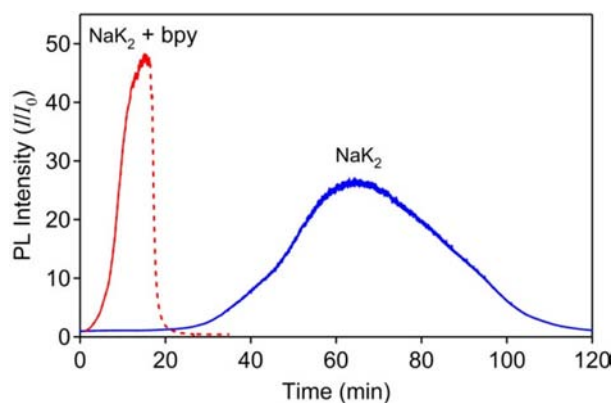


**Figure 2.** Traces of the time evolution of the chemical brightening for colloidal  $\text{Mn}^{2+}:\text{ZnSe}$  nanocrystals ( $1.3 \times 10^{-6}$  M;  $d = 4.6$  nm) with  $\text{NaK}_2$  (blue) or  $\text{NaK}_2$  plus 2,2'-bipyridine (red). The PL intensity ( $I$ ) is plotted in terms of multiples of the original intensity ( $I_0$ ). Exposure to air rapidly reverses the PL brightening (dashed).

the NCs slowly precipitated, and the PL was eventually lost (Figure 2). To improve the reduction kinetics, 2,2'-bipyridine (bpy) was introduced as a molecular electron shuttle. This addition not only caused a 6-fold acceleration of the brightening but also yielded a  $\sim 2$ -fold increase in the maximum PL relative to  $\text{NaK}_2$  alone. As with the  $\text{NaK}_2$  reaction, the PL of these NCs was not stable, and slowly decreased again after reaching maximum brightening, although the PL change became difficult to monitor because of absorption at the same energies from accumulating bpy radical (data not shown). Exposing the brightened solution to ambient atmosphere resulted in rapid PL loss (Figure 2), confirming the redox nature of the transformation. These results demonstrate the importance of reducible surface states in freestanding colloidal NCs as well as the concept of targeted chemical delivery of redox equivalents to the surfaces of such NCs.

Electrochemical studies of  $\text{Mn}^{2+}:\text{ZnSe}$  NC films showed reduction starting as low as  $\sim 1.2$  V below the conduction-band minimum and increasing gradually at more cathodic potentials, suggesting broadly distributed surface-state potentials.<sup>25</sup> To probe the distribution of traps in the colloidal NCs, electrons were titrated into stirring solutions of  $\text{Mn}^{2+}:\text{ZnSe}$  NCs using molecular reductants with different redox potentials. Titration of bis(cyclopentadienyl)cobalt(II) [cobaltocene,  $-1.3$  V vs the ferrocene (Fc)/ferrocenium ( $\text{Fc}^+$ ) couple<sup>26,27</sup>] led to escalating PL before eventual saturation at  $\sim 10$ -fold brightening (to  $\phi_{\text{max}} = 4\%$ ) with  $\sim 350$  equiv. We hypothesized that the smaller brightening here compared with Figure 2 is related to the fact that the redox potential of cobaltocene is insufficient to reduce some surface traps. This hypothesis was confirmed by switching to anthracene radical as the reductant,<sup>28</sup> which has a redox potential of  $-2.5$  V vs  $\text{Fc}/\text{Fc}^+$ .<sup>26</sup> For up to  $\sim 225$  equiv, anthracene radical induced an almost identical 4-fold PL brightening as cobaltocene (Figure 3). Beyond this amount, however, anthracene radical addition accelerated the PL brightening relative to cobaltocene, eventually maximizing at a  $\sim 33$ -fold increase (to  $\phi_{\text{max}} = 13\%$ ) with  $\sim 400$  equiv of reductant. These results demonstrate that the potential of the supplied electron dictates the magnitude of the PL enhancement, thereby implicating a broad distribution of reducible trap potentials in these colloidal NCs. The absence of any detectable changes in the absorption spectra during the course of these experiments (Figure S1 in the SI) eliminated nanocrystal

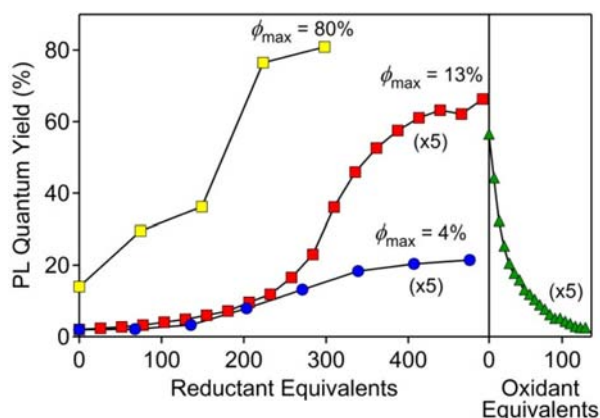


**Figure 3.** Changes in  $\text{Mn}^{2+} \ ^4\text{T}_1 \rightarrow \ ^6\text{A}_1$  PL quantum yield in colloidal  $\text{Mn}^{2+}:\text{ZnSe}$  NCs ( $2.6 \times 10^{-7}$  M;  $d = 4.6$  nm) vs equivalents of reductant or oxidant. Data for reduction of as-prepared NCs by cobaltocene (blue  $\bullet$  [ $\phi_{\text{initial}} = 0.4\%$ ]) and anthracene radical (red  $\blacksquare$  [ $\phi_{\text{initial}} = 0.4\%$ ] and yellow  $\blacksquare$  [ $\phi_{\text{initial}} = 14\%$ ]) and for oxidation of maximally brightened NCs by BAHA (green  $\blacktriangle$ ) are shown. The data for NCs with initial quantum yields of 0.4% have been multiplied by 5 for clarity.

etching, growth, or conduction-band filling as possible origins of the redox brightening. In contrast with the NCs subjected to a continuous source of reductant (Figure 2), NCs reduced by titration remained stable against precipitation, indicating that the effectively unlimited reducing capacity of the vast excess of  $\text{NaK}_2$  used for Figure 2 caused the NC precipitation.

Interestingly, the saturation of the redox brightening in Figure 3 occurred at reductant:NC ratios of at least 300:1 (i.e., a large excess of reductant). The contrast between the extent of reductant required here and that estimated for QD electro-brightening [ $I/I_0(\text{max})$  at greater than  $\sim 10$  electrons/NC]<sup>25</sup> may reflect either the importance of increased surface area and ligand mobility in colloidal suspensions or the difference between stoichiometric and steady-state reducing conditions. Moreover, brightening occurred only following what resembled an induction stage, where initial reductant aliquots produced less PL increase than later aliquots. These results could indicate that impurities (e.g., trace  $\text{O}_2$ , water, or excess NC ligand) intercepted some of the reducing equivalents. Alternatively, they could reflect a large surface capacitance and a nonlinear PL response to progressive trap passivation. To test the possibility that this induction period was somehow related to the small initial PL quantum yields of these NCs, experiments were next performed using NCs with larger initial quantum yields ( $d = 3.8$  nm, 1%  $\text{Mn}^{2+}$ ;  $\phi = 14\%$ ). Redox-brightening data collected using anthracene radical as the reductant are included in Figure 3. Not only was less reductant needed to achieve maximum brightening ( $\phi_{\text{max}} = 80\%$  at  $\sim 300$  electrons/NC,  $I/I_0 = 5.7$ ), but the data also no longer showed a similar induction stage before the PL increased. The two experiments were performed under essentially identical conditions, arguing against attribution of the induction stage in the low-quantum-yield NCs to spurious oxidants. Instead, the data suggest that reduction of the deepest traps occurs without significant PL improvement. The nonlinear PL response to added reducing equivalents is thus consistent with the conclusion that the largest PL increase per added electron comes when the number of remaining traps is smallest (Figure S2).

As an independent test, the outer-sphere one-electron oxidant tris(4-bromophenyl)aminium hexachloroantimonate

(BAHA) was titrated against a reductively brightened colloidal suspension of the low-quantum-yield  $\text{Mn}^{2+}:\text{ZnSe}$  NCs used in Figure 2. The NC PL approached its initial value upon removal of  $\sim 100$  electrons/NC (Figure 3, right),  $\sim 4$  times fewer electrons than had been added but comparable to the number of electrons needed to span the same range of PL intensities in the other direction. These data are consistent with the conclusion that the low-quantum-yield reductive brightening shown in Figure 3 involves at least 100 reduction events per NC. Although this number appears to be large, it is comparable to the number of unpassivated surface sites estimated for these NCs, or the number of coordinating ligands. For a  $d = 4.6$  nm NC, approximately one-quarter of the ZnSe is at the surface, which would correspond to  $\sim 250$  ZnSe units. Typical packing densities of TOPO may provide  $\sim 30\%$  surface coverage,<sup>17</sup> meaning  $\sim 75$  surfactant ligands and  $\sim 175$  unpassivated surface binding sites would be present [i.e., sufficient capacity to accommodate the electrons provided by the chemical reductants plus cations (e.g.,  $\text{Na}^+$  or  $\text{K}^+$ ) to compensate for the additional charge]. Regardless of the precise numbers, well beyond stoichiometric quantities of reductant are required for maximum redox brightening of both the low- and high-quantum-yield NCs.

In all of the samples, the PL decreased slowly after reductive brightening (Figure S2), possibly because of the slow introduction of adventitious oxygen or interactions of the reduced NCs with other molecules in solution. This PL decrease was greatly accelerated by air (Figure 2), demonstrating that reductive trap passivation under these conditions is easily reversed by exposure to oxidants. Whereas surface-trap reduction can form high-quantum-yield ZnSe-based NCs, stabilization of these high quantum yields must be accomplished by independent means. Such experiments are presently underway.

The results presented here demonstrate redox brightening of freestanding colloidal  $\text{Mn}^{2+}:\text{ZnSe}$  NCs via the addition of noncoordinating molecular reductants. The potential of the reductant determines the extent of redox brightening. Titration showed that the brightening is associated with multiple reducing equivalents per NC, which can be rationalized by consideration of the large surface-to-volume ratios and imperfect surface passivation of these NCs. These results highlight the importance of surface electron traps in the PL of colloidal ZnSe-based NCs. Understanding the microscopic origins of redox brightening in this model system will be generally informative because of the paucity of molecular-level information about surface traps and may enable extension to other related NCs where redox-active surfaces inhibit performance. Future experiments will therefore focus on characterizing the microscopic identities of the redox-active traps and on the development of chemical methods for making this brightening robust against reversal by air.

## ■ ASSOCIATED CONTENT

### Supporting Information

Synthetic and experimental data and additional analysis. This material is available free of charge via the Internet at <http://pubs.acs.org>.

## ■ AUTHOR INFORMATION

### Corresponding Author

[gamelin@chem.washington.edu](mailto:gamelin@chem.washington.edu)

## Notes

The authors declare no competing financial interest.

## ■ ACKNOWLEDGMENTS

Financial support from the U.S. National Science Foundation (DMR-1206221), the Research Corporation, and the University of Washington is gratefully acknowledged.

## ■ REFERENCES

- (1) Shim, M.; Guyot-Sionnest, P. *Nature* **2000**, *407*, 981–983.
- (2) Shim, M.; Wang, C.; Guyot-Sionnest, P. *J. Phys. Chem. B* **2001**, *105*, 2369–2373.
- (3) Liu, W. K.; Whitaker, K. M.; Smith, A. L.; Kittilstved, K. R.; Robinson, B. H.; Gamelin, D. R. *Phys. Rev. Lett.* **2007**, *98*, No. 186804.
- (4) Whitaker, K. M.; Ochsenein, S. T.; Polinger, V. Z.; Gamelin, D. R. *J. Phys. Chem. C* **2008**, *112*, 14331–14335.
- (5) Nirmal, M.; Murray, C. B.; Bawendi, M. G. *Phys. Rev. B* **1994**, *50*, 2293–2300.
- (6) Hines, M. A.; Guyot-Sionnest, P. *J. Phys. Chem.* **1996**, *100*, 468–471.
- (7) Kuno, M.; Lee, J. K.; Dabbousi, B. O.; Mikulec, F. V.; Bawendi, M. G. *J. Chem. Phys.* **1997**, *106*, 9869–9882.
- (8) Burda, C.; Link, S.; Mohamed, M.; El-Sayed, M. *J. Phys. Chem. B* **2001**, *105*, 12286–12292.
- (9) Wuister, S. F.; de Mello Donegá, C.; Meijerink, A. *J. Phys. Chem. B* **2004**, *108*, 17393–17397.
- (10) Kalyuzhny, G.; Murray, R. W. *J. Phys. Chem. B* **2005**, *109*, 7012–7021.
- (11) Chen, Y.; Vela, J.; Htoon, H.; Casson, J. L.; Werder, D. J.; Bussian, D. A.; Klimov, V. I.; Hollingsworth, J. A. *J. Am. Chem. Soc.* **2008**, *130*, 5026–5027.
- (12) Geyer, S.; Porter, V. J.; Halpert, J. E.; Mentzel, T. S.; Kastner, M. A.; Bawendi, M. G. *Phys. Rev. B* **2010**, *82*, No. 155201.
- (13) Dabbousi, B. O.; Rodriguez-Viejo, J.; Mikulec, F. V.; Heine, J. R.; Mattoussi, H.; Ober, R.; Jensen, K. F.; Bawendi, M. G. *J. Phys. Chem. B* **1997**, *101*, 9463–9475.
- (14) Mahler, B.; Spinicelli, P.; Buil, S.; Quelin, X.; Hermier, J.-P.; Dubertret, B. *Nat. Mater.* **2008**, *7*, 659.
- (15) Wang, X.; Ren, X.; Kahen, K.; Hahn, M. A.; Rajeswaran, M.; Maccagnano-Zacher, S.; Silcox, J.; Cragg, G. E.; Efros, A. L.; Krauss, T. D. *Nature* **2009**, *459*, 686–689.
- (16) Qu, L. H.; Peng, X. G. *J. Am. Chem. Soc.* **2002**, *124*, 2049–2055.
- (17) Bullen, C.; Mulvaney, P. *Langmuir* **2006**, *22*, 3007–3013.
- (18) Jasieniak, J.; Mulvaney, P. *J. Am. Chem. Soc.* **2007**, *129*, 2841–2848.
- (19) Munro, A. M.; Jen-La Plante, I.; Ng, M. S.; Ginger, D. S. *J. Phys. Chem. C* **2007**, *111*, 6220–6227.
- (20) Duncan, T. V.; Polanco, M. A. M.; Kim, Y.; Park, S.-J. *J. Phys. Chem. C* **2009**, *113*, 7561–7566.
- (21) Evans, C. M.; Cass, L. C.; Knowles, K. E.; Tice, D. B.; Chang, R. P. H.; Weiss, E. A. *J. Coord. Chem.* **2012**, *65*, 2391–2414.
- (22) Jha, P. P.; Guyot-Sionnest, P. *J. Phys. Chem. C* **2010**, *114*, 21138–21141.
- (23) Galland, C.; Ghosh, Y.; Steinbrück, A.; Sykora, M.; Hollingsworth, J. A.; Klimov, V. I.; Htoon, H. *Nature* **2011**, *479*, 203–207.
- (24) Qin, W.; Shah, R. A.; Guyot-Sionnest, P. *ACS Nano* **2012**, *6*, 912–918.
- (25) Weaver, A. L.; Gamelin, D. R. *J. Am. Chem. Soc.* **2012**, *134*, 6819–6825.
- (26) Connelly, N. G.; Geiger, W. E. *Chem. Rev.* **1996**, *96*, 877–910.
- (27) All potentials quoted are for glyme solutions. Significant variation is not expected for the THF solutions used in the present work.
- (28) The anthracene radical was generated by  $\text{NaK}_2$  reduction of anthracene in THF.